Development of Unique Test Bed for Assessing Stability Response of Steel Cantilevered Girders

Maha Essa, Vahab Esmaeili, Ali Imanpour, and Robert Driver

Abstract Cantilever-suspended-span construction, also known as the Gerber system, is a popular framing scheme used for roofs of large single-storey buildings in North America. Despite their advantages and widespread application, collapses of Gerber roofs have made it clear that there are stability issues implicit in these systems that are not reflected as part of a unified design method. It is, therefore, necessary to understand the complex stability response of these systems—which can benefit greatly from the results of full-scale physical testing of overhanging girders. This paper outlines the development of a test bed for evaluating the stability response of overhanging girders and an experimental plan for the stability assessment of Gerber systems, which represents a part of an ongoing comprehensive research project at the University of Alberta. The primary criteria for the selection of the test specimens are first introduced. A finite-element model is then utilized to highlight the importance of those criteria through several numerical simulations. The key considerations of the test setup design, including the loading and lateral bracing conditions as well as restraints at column locations, are discussed. Simulating proper boundary conditions is of crucial importance in the experimental study of overhanging girders. The results reveal that the existence or absence of bottom chord extensions for secondary members, typically open-web steel joists, is a key design consideration for the test setup and can be highly influential in the stability response of the Gerber system.

Keywords Test bed · Stability response · Steel cantilevered girders

1 Introduction

Cantilever-suspended-span construction, also known as the Gerber system, is a common roof framing scheme for large single-storey buildings in North America. This system, shown in Fig. 1, consists of a series of simply supported girders in

M. Essa (✉) · V. Esmaeili · A. Imanpour · R. Driver
University of Alberta, Edmonton, AB, Canada
e-mail: essa@ualberta.ca

© Canadian Society for Civil Engineering 2023

R. Gupta et al. (eds.), *Proceedings of the Canadian Society of Civil Engineering Annual Conference 2022*, Lecture Notes in Civil Engineering 348,
https://doi.org/10.1007/978-3-031-34159-5_12

Fig. 1 Gerber system in a single-storey building in Edmonton, AB

the principal framing direction that extend beyond the column as cantilevers, with open-web steel joists (OWSJs) as the secondary framing members. Drop-in spans are supported in alternate bays at the cantilever ends. The continuity between adjacent bays results in lower magnitudes of positive moment by introducing negative moments at the supports. As a result of the balanced moments, Gerber girders allow for a more efficient design—where lighter and shallower girders are adequate to carry the same loads as compared to simply supported spans. Furthermore, the system avoids costly and complex moment connections, making it faster to erect, and results in lower deflections than those seen in conventional roof girders [11].

Despite the advantages and widespread application of the Gerber system in steel buildings in North America, current steel design standards in Canada and the United States [1, 5] provide little guidance on the design of Gerber systems—especially with regard to the effect of the interaction between the cantilever and the back span on lateral–torsional buckling (LTB) of the system. The prediction of the LTB response in this system relies on the consideration of a variety of parameters, including loading and bracing conditions. The effects of these parameters can be realized from the results of full-scale physical testing of overhanging girders subject to different bracing and loading conditions. This paper outlines the development of a unique test bed for evaluating the stability response of overhanging girders used in Gerber systems. The experimental data obtained from these tests will be used to further validate a comprehensive finite-element model for overhanging girders developed as part of an ongoing research project at the University of Alberta [7]. The accurate validation of this model will be instrumental in developing a practical design method in the framework of the Canadian steel design standard for cantilevered girders.

2 Gerber Stability Database

As part of the larger research project, a comprehensive finite-element model [7] has been developed in the *Abaqus* programme [6] for overhanging girders. In addition to global buckling limit state, the possibility of distortional buckling—where the girder cross-section undergoes distortion and deflection simultaneously—greatly influences

the flexural capacity of overhanging girders [9]. The finite-element model is capable of considering such buckling modes, as well as material and geometric nonlinearities, initial geometric imperfections, and residual stresses.

Figure 2 shows the configuration of a typical overhanging girder considered in this study. In this figure, P_b refers to the point loads on the back span coming from OWSJs; $P_{\max}$ and $P_{\min}$ represent the larger and smaller point loads at the cantilever tips, respectively; L_b denotes the length of the back span; L_c is the length of the cantilever; s represents the joist spacing; n equals the number of point loads on the back span plus 1; $M^l_{\max}$ is the local maximum bending moment along the back span; $M_{F_{\max}}$ and $M_{F_{\min}}$ signify the bending moments at the two supports; and κ'_1 and κ'_2 are defined as $\frac{M^l_{\max}}{M_{F_{\max}}}$ and $\frac{M_{F_{\min}}}{M_{F_{\max}}}$, respectively.

A total of 266 overhanging girders, including 245 single-overhanging girders and 21 double-overhanging girders, are considered in the numerical simulation. These include seven standard steel wide-flange sections (W-shapes), which conform to both CSA G40.21 Grade 345WM [4] and ASTM A992 [2]. The cross-sectional properties and class [5] of the selected cross-sections are presented in Table 1. For all the girders, the length of the back span, L_b, is 9.0 m and the length of the cantilever, L_c, and joist spacing, s, are both equal to 1.8 m.

In Table 1, $b/2t$ represents the flange slenderness ratio, where b is the overall width of the flange and t denotes its thickness; h/w is the web slenderness ratio, where h is the clear depth of the web and w denotes its thickness; I_x/I_y is an index of the difference between the strong- and weak-axis geometric stiffnesses of the girder; and d is the depth of the section.

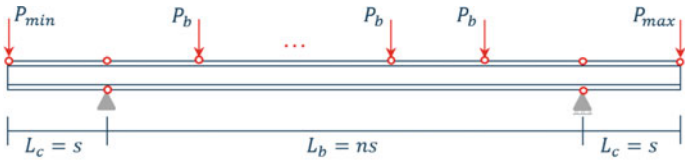

(a) Configuration

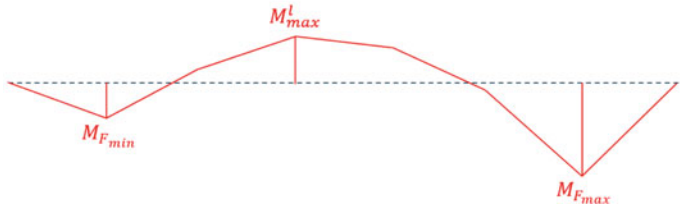

(b) Bending moment diagram

Fig. 2 Typical overhanging girder (symbol red circle represents point of lateral support)

Table 1 Geometrical properties of selected cross-sections

Cross-section	Flange class	Web class	$\frac{b}{2t}$	$\frac{h}{w}$	$\frac{I_x}{I_y}$	$\frac{L_b}{d}$
W410 × 85	1	1	5.0	34.8	17.5	22
W460 × 52	1	1	7.0	56.4	33.4	20
W460 × 60	1	1	5.8	53.6	32.0	20
W460 × 97	1	1	5.1	37.5	19.5	19
W460 × 144	1	1	6.4	31.5	8.7	19
W530 × 66	1	1	7.2	56.4	41.0	17
W530 × 82	2	1	7.9	52.8	23.5	17

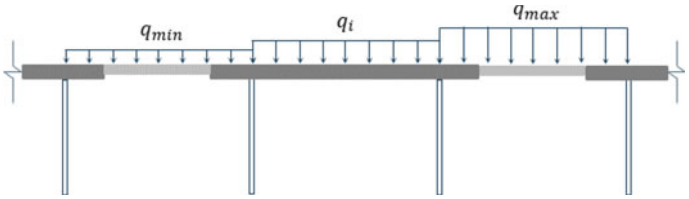

Fig. 3 Typical roof framing under a schematic load pattern

Figure 3 shows a typical roof framing under a schematic load pattern. This highlights the importance of considering pattern loading in the study, which can occur due to phenomena such as moving live loads or drifting snow.

In Fig. 3, q_i refers to the distributed load on the back span bay; $q_{\max}$ and $q_{\min}$ represent the larger and smaller distributed loads on the adjacent bays, respectively; and κ_1'' and κ_2'' are defined as $q_i/q_{\max}$ and $q_{\min}/q_{\max}$, respectively. To develop the Gerber stability database, the following range is considered for κ_1'':

$$\kappa_1'' = \{2.00, 1.60, 1.30, 1.00, 0.77, 0.63, 0.50\} \tag{1}$$

κ_2'' is equal to zero for single-overhanging girders considered in this study.

While the finite-element model has been validated using available test results [7], the experimental test programme outlined in this paper will evaluate experimentally a wider range of Gerber girders by varying configuration (single or double overhang), loading scheme, and cross-section to achieve a better representation of the stability of such girders. The data from these tests will then be used to further validate the numerical model.

3 Test Specimen Selection Criteria and Matrix

The finite-element model described earlier is used to evaluate the influence of various parameters on the lateral–torsional buckling capacity of steel cantilevered girders. These parameters include configuration (single or double overhang), cross-sectional properties, loading conditions, and lateral bracing conditions. The parameters with the highest influence according to the numerical simulations [7] are to be considered so as to select test specimens, which will expand on the existing cantilever test database provided by [8].

The specimens are categorized into five distinct groups according to the restraint conditions on the cantilever and back span, as shown in Fig. 4, with the following identifiers:

Single-overhanging girders	
LRC 1: C(T) – B(T)	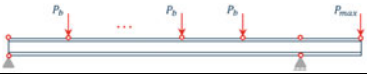
LRC 2: C(U) – B(T)	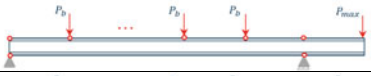
LRC 3: C(U) – B(TB)	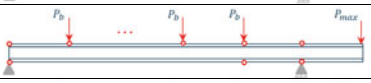
LRC 4: C(TB) – B(T)	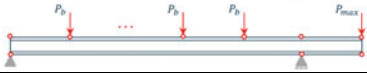
LRC 5: C(TB) – B(TB)	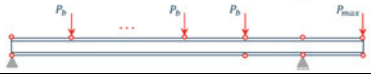
Double-overhanging girders	
LRC 1: C(T) – B(T)	
LRC 2: C(U) – B(T)	
LRC 3: C(U) – B(TB)	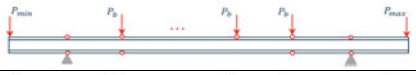
LRC 4: C(TB) – B(T)	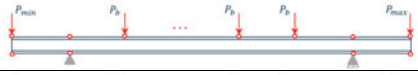
LRC 5: C(TB) – B(TB)	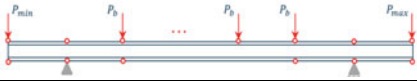

Fig. 4 Test specimen loading and restraint conditions

- $C(T) - B(T)$: cantilever tip is laterally restrained at the top flange and back span is laterally restrained at the top flange;
- C(U) – B(T): cantilever tip is unbraced and back span is laterally restrained at the top flange;
- C(U) – B(TB): cantilever tip is unbraced and back span is laterally restrained at both the top and bottom flanges;
- C(TB) – B(T): cantilever tip is laterally restrained at both the top and bottom flanges and back span is laterally restrained at the top flange; and
- C(TB) – B(TB): cantilever tip is laterally restrained at both the top and bottom flanges and back span is laterally restrained at both the top and bottom flanges.

3.1 Configuration

While the tests performed by [8] were limited to only single-overhanging girders, this experimental study will incorporate both single and double-overhanging girders. In practice, both configurations are used in the Gerber system depending on the location of the cantilever segment in the structural layout. While end spans typically consist of single-overhanging girders, interior spans typically consist of girders that run continuously over two columns in a double-overhanging configuration then connecting to drop-in segments on either end. It is therefore important to understand the stability response of both configurations of overhanging girders.

The proposed test specimen configurations consisted of single-overhanging girders with a total length of 10.8 m and double-overhanging girders having a total length of 12.6 m. This length includes the lengths beyond the support centreline and cantilever tip load centreline.

The numerical model was used to assess the effects of different L_b/d ratios on the nominal capacity of the girder, M_n, for both single and double-overhanging girders. This was achieved by varying κ_1'' values, namely, 0.625, 1, and 1.6. The results of the analyses for Group $C(T) - B(T)$ are shown in Fig. 5.

The configuration is seen to have a significant impact on the capacity of the system, with the additional cantilever on the double-overhanging girders having the ability to either increase or decrease the moment capacity depending on the load pattern ratios. The smaller capacities seen for double-overhanging girders are a result of smaller κ_1' values for the same κ_1'' values as a single-overhanging girder. Furthermore, the peaks in the chart correspond to the sections in Table 1 with smaller I_x/I_y values (W410 $\times$ 85, W460 $\times$ 97, and W460 $\times$ 144), and are consequently stronger than the rest of the sections in terms of weak-axis bending. It is therefore crucial to investigate both configurations to fully capture the stability response of Gerber systems.

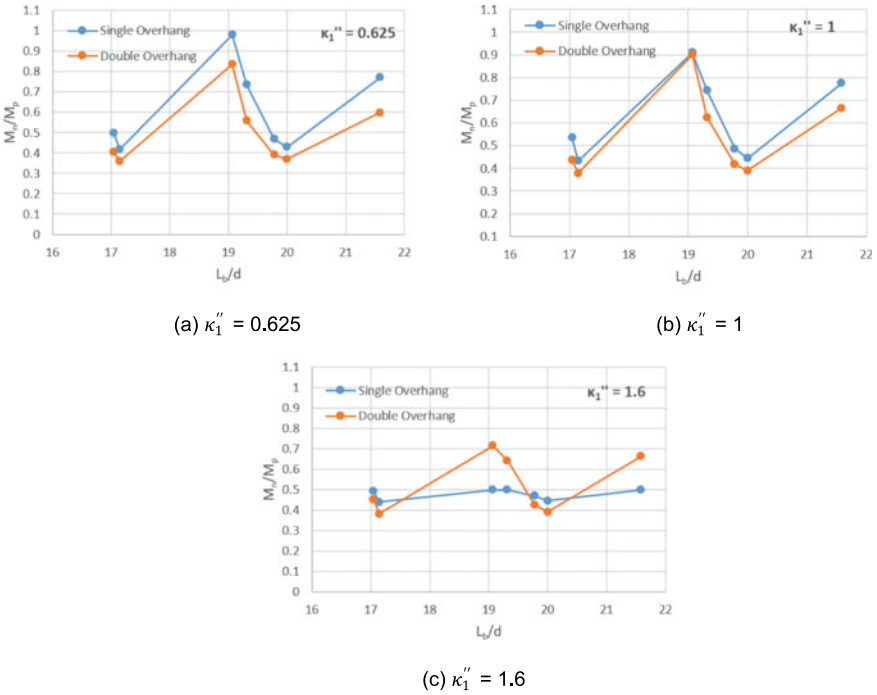

Fig. 5 Effect of configuration on nominal capacity for the $C(T) - B(T)$ group

3.2 *Cross-Sectional Properties*

The experimental programme performed by [8] was limited to two cross-sections, W360 × 39 and W310 × 39, both of which are considered in today's Gerber construction practice as shallow and light, but were primarily selected to meet the laboratory constraints. To expand on this, the proposed test matrix of this experimental study includes three new cross-sections: W410 × 85, W310 × 44.5, and W460 × 113. The W410 × 85 section complies with the Class 1 section width-to-thickness ratio limits, and the W310 × 44.5 and W460 × 113 profiles meet Class 2 section requirements.

The selection of these three cross-sections was based on the results of the numerical simulations [7] that show that dimensionless parameters $b/2t$ (flange width-to-thickness ratio or local slenderness ratio) and I_x/I_y (ratio of moments of inertia) are particularly influential on the lateral–torsional buckling capacity of cantilever girders. The nominal values of both parameters for each cross-section is presented in Table 2.

Numerical simulation results can be used to realize the significance of cross-sectional properties on the nominal flexural capacity, M_n, of overhanging girders. Figure 6 shows the variation of the nominal capacity as I_x/I_y changes for the $C(T) - B(T)$ group.

Table 2 Flange local slenderness ratio and ratio of moments of inertia for selected wide-flange sections

Gerber girder	$\frac{b}{2t}$	$\frac{I_x}{I_y}$
W410 × 85	4.97	17.5
W310 × 44.5	7.41	11.6
W460 × 113	8.09	8.78

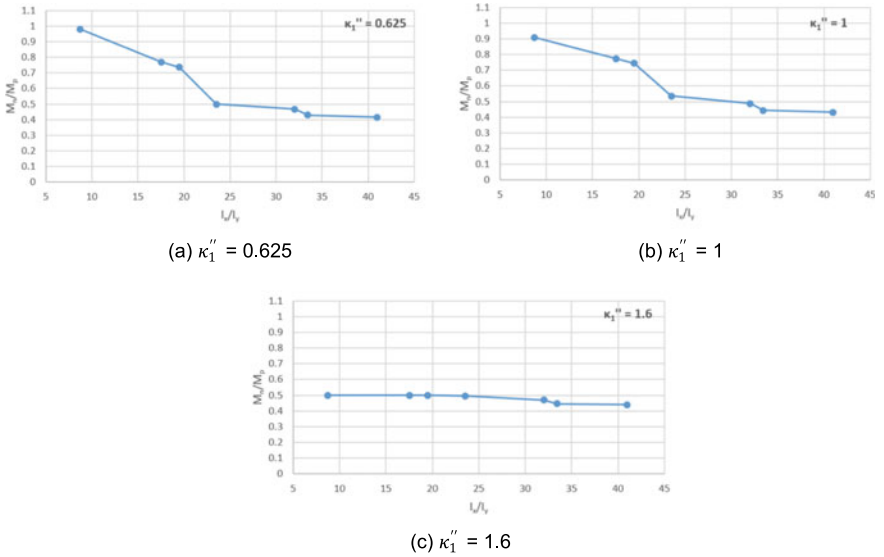

(a) $\kappa_1^{''}$ = 0.625 (b) $\kappa_1^{''}$ = 1

(c) $\kappa_1^{''}$ = 1.6

Fig. 6 Effect of cross-sectional properties on the flexural capacity of cantilevered girders for the $C(T) - B(T)$ group

As seen in the numerical simulation results, the capacities of the sections are greatly influenced by the cross-sectional properties. Increasing the $\frac{I_x}{I_y}$ ratio indicates that the moment of inertia about the weak-axis, I_y, is decreasing relative to the moment of inertia about the strong axis, I_x. This causes the system to be more susceptible to lateral–torsional buckling, which explains the decrease in capacity as this ratio increases and highlights the importance of testing various cross-sections.

3.3 Loading Condition

Another parameter that was identified from the numerical simulations as having a high impact on the stability of the system, particularly the stability of the back span, is the shape of the bending moment diagram. This is quantified by the ratio $\kappa_1^{'} = M_{\max}^{l}/M_{F_{\max}}$, where $M_{\max}^{l}$ is the local maximum bending moment on the back span, and $M_{F_{\max}}$ is the bending moment at the support. Due to the continuity of the

Table 3 Variation of κ_1''' and κ_1' considered in test programme

κ_1'''	κ_1'
0.80	− 1.90
0.50	− 1.00
0.31	− 0.44

girder over the column, the negative moment at the column causes the bottom flange of the girder to go into compression. The length of the bottom flange under compression and the location of inflection points depends on the bending moment gradient, and therefore the loading condition. For this reason, it is important to evaluate the system under pattern loading. This is reproduced in the proposed experimental study by testing the girders under different load ratios. The loading of the test specimens involve four point loads at 1.8-m intervals on the 9 m-long back span plus a point load applied at the tip of the 1.8 m-long cantilever. A distinct load of $P_{\max}$ will be applied on the cantilever tip in each of the tests of all test specimen groups. The load on the back span, P_b, will then be varied in each of the tests with respect to $P_{\max}$ until a desired κ_1' ratio is achieved, as shown in Table 3. This is quantified by the ratio $\kappa_1''' = P_b/P_{\max}\kappa_1'$, which can take on three values: 0.80, 0.50, or 0.31. Table 3 summarizes the variation of κ_1''' considered in the tests and their corresponding κ_1' values.

Numerical simulation results showed the influence of different load patterns, quantified by κ_1'' in the context of the numerical simulations, on the nominal flexural capacity of the girder. Figure 7 shows this effect for the three cross-sections in the C(T)–B(T) group.

For a single-overhanging girder, increasing the κ_1'' value represents increasing the load on the back span compared to the load on the cantilever. Referring to the numerical results, increasing κ_1'' past a value of 1.00 (corresponding to a higher load on the back span than on the cantilever) leads to a rapid decrease in the moment capacity of the section. Therefore, loading conditions are of crucial significance when investigating the capacity of an overhanging girder, and therefore various loading conditions have been included in the selection criteria of the test matrix.

3.4 Lateral Bracing Condition

The cantilever portion of a Gerber system can be subject to various bracing conditions in the real world, which is being simulated in this experimental study by including the test specimen groups introduced earlier (Fig. 4). The Gerber stability database confirmed that different bracing conditions at the cantilever tip, as well as the presence of a bottom chord extension on secondary members off the column line, have a significant impact on the capacity of the system.

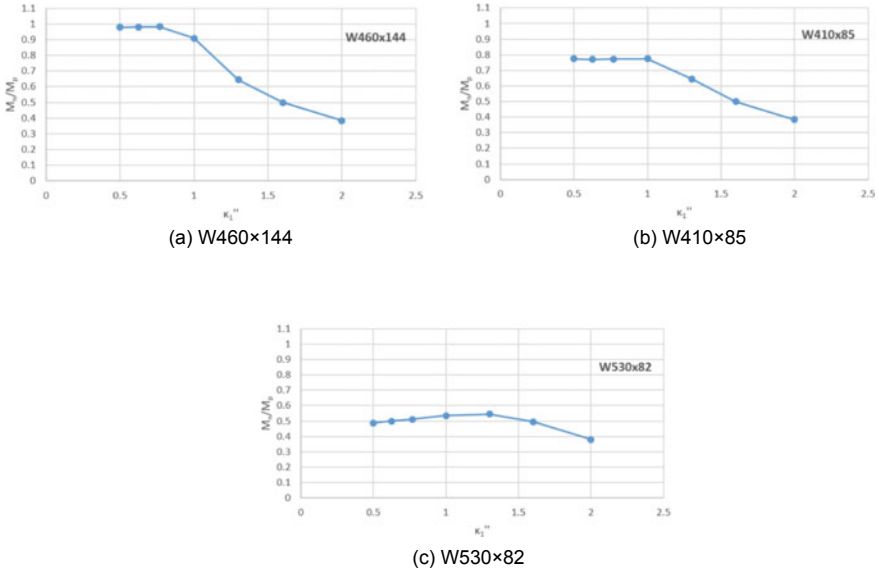

(a) W460×144 (b) W410×85

(c) W530×82

Fig. 7 Effect of load pattern on nominal flexural capacity for the C(T)–B(T) group

The numerical model was used to analyse the effect of different L_b/d ratios on the nominal flexural capacity of the girder, M_n, for the test specimen groups as shown in Fig. 8. This was achieved by varying κ_1'' values, namely, 0.625, 1, and 1.6.

The numerical results showed that the models with bottom chord extensions at the bracing location off the column line exhibit a significantly higher capacity compared to the models where only the top flange is braced along the entire back span. Due to the variation in capacity with varying bracing conditions, the inclusion of various lateral bracing conditions in the test matrix is essential.

4 Test Bed Design

The experimental test programme described in this paper consists of 15 W410 × 85 single-overhanging girders. The ongoing design of the test setup is being done by paying consideration to minimizing incidental restraint, which can have a significant impact on the results of large-scale experimental testing by resulting in capacities higher than what would have been obtained under the intended restraint [15]. The test setup design considerations are based largely on the recommendations of the Structural Stability Research Council (SSRC) Technical Memorandum No. 9 on flexural testing [15]. Models have been prepared in *Revit* [3] for each of the five test specimen groups. Figure 9 shows the overall test setup for the C(T)–B(T) case. In this figure, the blue member is the test specimen, and the load frame, bracing system and

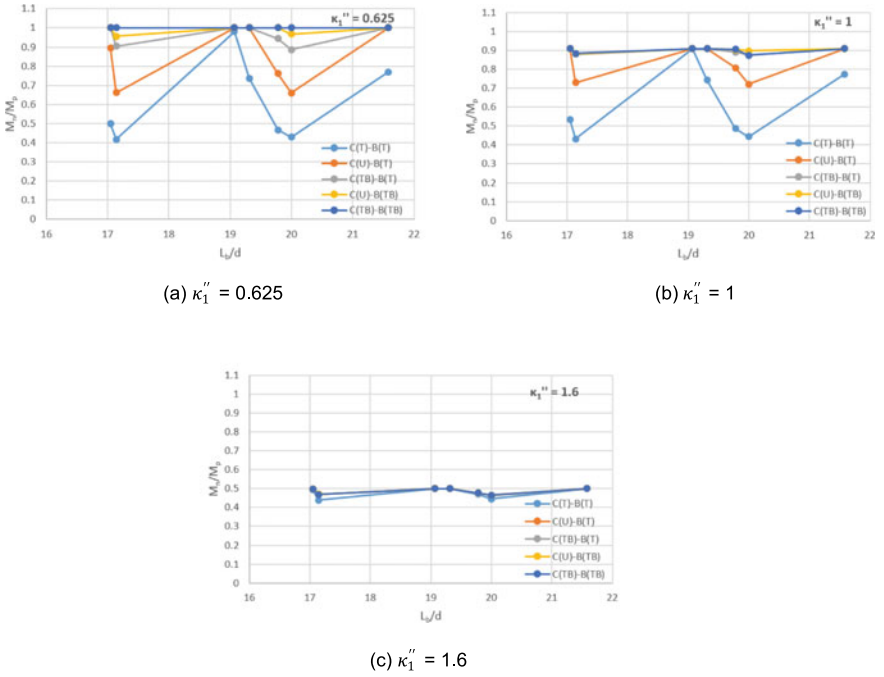

(a) κ_1'' = 0.625

(b) κ_1'' = 1

(c) κ_1'' = 1.6

Fig. 8 Effect of lateral bracing condition on flexural capacity of single-overhanging girders

supports are shown in grey. This section describes the loading, support, and bracing details of the test setup to simulate those anticipated in a typical Gerber system.

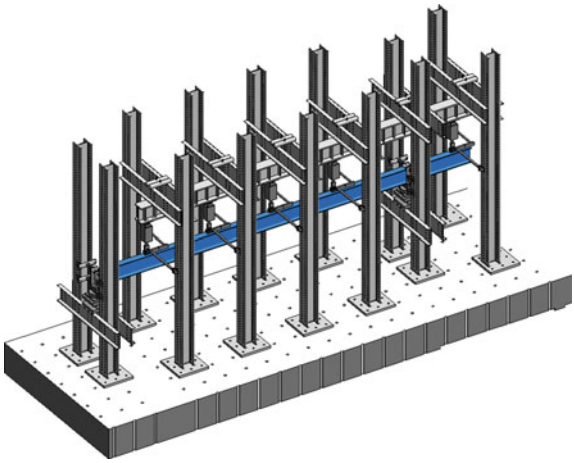

Fig. 9 Model of test setup for C(T)–B(T) case (test specimen shown in blue)

4.1 Physical Simulation of Loading Conditions

The loading of the test specimens involve four point loads at 1.8-m intervals on the 9 m-long back span plus a point load applied at the tip of the 1.8 m-long cantilever. The gravity load is applied using a hydraulic actuator, which generates the concentrated load on test specimen. On one end, the hydraulic actuators are connected to a stiff reaction frame composed of a distributing beam connected to 2.7 m-long MC 460 × 86 channels, which subsequently span across two 6 m-tall columns on either side of the girder. At the opposite end, the actuator is connected to a semi-cylindrical bearing with its axis aligned with the longitudinal axis of the girder, which accommodates cross-section twist and sits on the top flange of the girder. This configuration is used at the load application points on both the back span and the cantilever in the test specimen groups where the cantilever tip is braced.

For the C(U)–B(T) and C(U)–B(TB) test specimen groups, where the cantilever tip is unbraced, a different gravity load application mechanism is employed which is composed of: (1) gravity load simulator (GLS), (2) hydraulic actuator, and (3) load collar. This configuration is shown in Fig. 10.

The gravity load simulator (GLS) is a mechanism designed to allow an applied load to remain vertical on a test specimen as the loaded structure undergoes sidesway [14]. Under an applied load provided by a hydraulic actuator, the GLS is able to move laterally by approximately 140–225 mm in either direction from its equilibrium position while keeping the hydraulic actuator vertical [10]. Therefore, employing the GLS at the cantilever tip when it is unbraced will effectively eliminate incidental restraint in the lateral direction while continuing to apply a vertical gravity load.

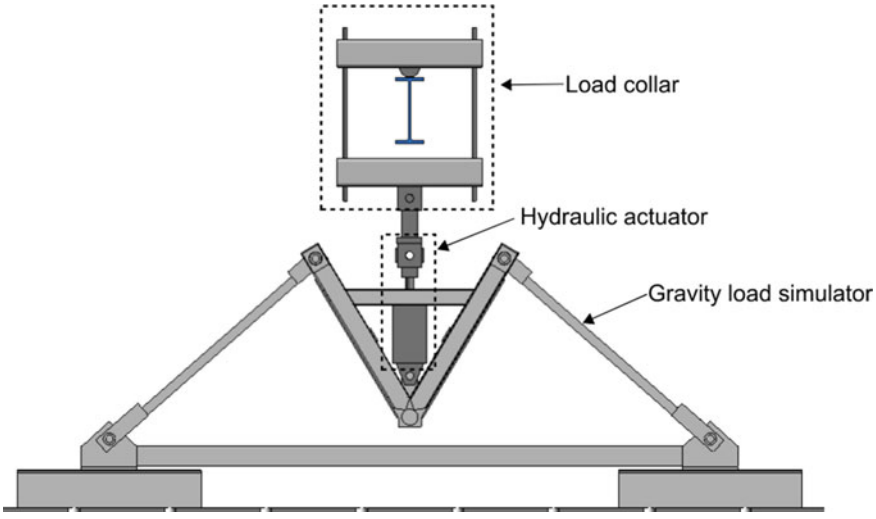

Fig. 10 Gravity load mechanism at an unbraced cantilever tip

The load collar, which surrounds the girder and is then connected to the hydraulic actuator through a yoke and tension rod, applies the load generated by the hydraulic actuator to the top flange of the girder. A semi-cylindrical bearing is also employed as part of the load collar in order to accommodate twisting of the cross-section.

4.2 Physical Simulation of Column Locations

Column locations in a typical Gerber frame are simulated in this experimental test setup at the supports. Identical configurations are used at the support fixtures at each end of the back span, resulting in the girder being simply supported. This means that the specimen is free to displace longitudinally and warp but is prevented from twisting and displacing laterally or vertically. To achieve this support condition, the specimen will rest on a set of rollers, a load cell, and a knife edge, as shown in Fig. 11. The rollers allow the girder to undergo longitudinal displacement, the knife edge allows the girder to pivot in-plane, and the load cell measures the reaction forces. These elements are supported on a pair of MC 460 × 86 channels spanning between two columns situated on either side of the girder.

Achieving a torsionally pinned boundary condition requires allowing the girder to warp, while preventing it from twisting. This is done by bringing in four lateral braces at each support, two which bear against the top flange and two against the bottom flange, effectively preventing cross-section twist and lateral movement of the girder. Furthermore, the girder is allowed to warp and displace longitudinally by equipping the lateral braces with rollers. The strength and stiffness requirements

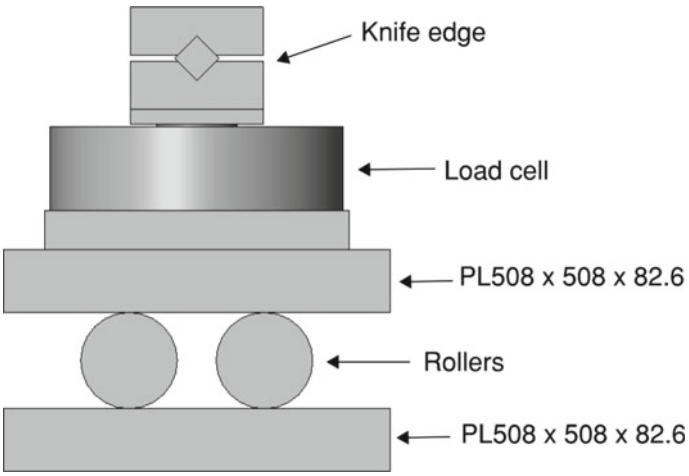

Fig. 11 Conceptual support detail

specified in Appendix 6 of AISC 360-16 [1] for girder point bracing are used to design lateral and torsional braces.

4.3 Physical Simulation of Lateral Bracing Conditions

Lateral bracing is used in flexural testing of girders to prevent out-of-plane movement. Since the girder is expected to deflect vertically along the back span and cantilever, in order to avoid incidental restraint it is important to use a lateral bracing mechanism that allows for free vertical movement while simultaneously restraining movement in the direction perpendicular to the girder web. Therefore, a conventional threaded rod, used at the supports as explained in Sect. 4.2, would not be appropriate for use at the load points. The lateral bracing condition in the test setup makes use of a Watt's linkage (Fig. 12), a type of brace which restrains lateral displacement while allowing for free translation in the longitudinal and vertical directions. The Watt's linkage has been used in previous lateral–torsional buckling tests [12–14]. As shown in Fig. 12, the Watt's linkage consists of two levers. One end of the lever is pin-connected to a column on one side of the girder (points A and B in Fig. 12), while the other end is pin-connected to a coupler (member CD in Fig. 12). The coupler includes a 1 ¼ in. diameter hole in the middle, through which the brace is pinned and welded to the flange of the girder being restrained.

Depending on the test specimen group, lateral bracing at various points along the back span may be provided to either the top flange only or both the top and bottom flanges. In cases where only the top flange is laterally restrained, only a single Watt's linkage would be used at the brace point, with the coupler connected to the top flange of the girder. For instance, a Watt's linkage would be connected to both the top and bottom flanges when simulating a bottom chord extension of a joist, effectively restraining the lateral movement of both flanges while allowing the girder to deflect vertically.

In the case of the cantilever tip, the load point may also be completely unbraced. The use of a gravity load simulator at the cantilever tip allows for a continuous gravity

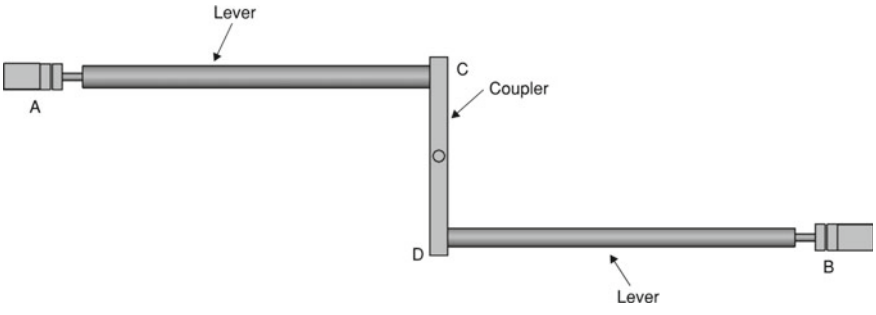

Fig. 12 Watt's linkage for lateral bracing

load application while allowing the specimen to undergo free lateral movement in either direction of its equilibrium position. By using the gravity load simulator in the C(U)–B(T) and C(U)–B(TB) groups, it is possible to apply an increasing point load while allowing the girder to deflect vertically and laterally, producing an unbraced cantilever tip. Meanwhile, Watt's linkages are still used at the brace points on the back span to restrain the top or bottom flange, as required.

5 Summary and Conclusions

An experimental test programme for evaluating the stability response of single-overhanging girders that aims to minimize incidental restraints and properly simulate the loading conditions, supports, and bracing conditions commonly used in Gerber construction is presented. A numerical database of the Gerber system developed in the companion study was used to select the test specimens and design the test setup. The experimental data obtained from the physical tests will be used to validate a comprehensive finite-element model which can predict the lateral–torsional buckling capacity for any arbitrary overhanging girder. This will be instrumental in proposing future design equations to be used in the design of Gerber girders.

Acknowledgements The support provided by the CISC Centre for Steel Structures Education and Research (the Steel Centre) at the University of Alberta is acknowledged. The authors hereby express their gratitude towards the industry advisors—Charles Albert, Elie Chakieh, Hesham Essa, Michael Holleran, Mark Lasby, Andy Metten, Samuel Richard, Elie Saint-Onge, Michael Samuels, and Alfred Wong—whose insightful inputs have enriched the work.

References

1. American Institute of Steel Construction (AISC) (2016) Specification for structural steel buildings (ANSI/AISC 360-16). Chicago, IL
2. American Society for Testing and Materials (ASTM) (2020) Standard specification for structural steel shapes. ASTM A992/A992M-20, ASTM, West Conshohocken, PA
3. Autodesk Inc. (2022) Revit architecture 2022 user's guide, Version 2022, San Rafael, CA
4. Canadian Standards Association (CSA) (2013) General requirements for rolled or welded structural quality steel/structural quality steel. CSA G40.20-13/G40.21-13 (reaffirmed 2018), CSA, Toronto, ON
5. Canadian Standards Association (CSA) (2019) Design of steel structures. CSA S16-19, CSA, Toronto, ON
6. Dassault Systèmes (2017) Abaqus/standard user's manual. Version 2017, Vélizy-Villacoublay, France
7. Esmaeili V, Imanpour A, Driver RG (2021) Stability of gerber systems with top-flange bracing. In: Proceedings of the annual stability conference. Structural Stability Research Council (SSRC). Louisville, KY
8. Essa HS, Kennedy DJ (1993) Distortional buckling of steel beams. Structural engineering report no. 185. University of Alberta, Edmonton, AB

9. Essa HS, Kennedy DJ (1994) Design of cantilever steel beams: refined approach. J Struct Eng 120(9):2623–2636
10. Ji D, Driver RG, Imanpour A (2019) Large-scale lateral–torsional buckling tests of welded girders. Steel centre engineering report no. 015. University of Alberta, Edmonton, AB
11. Rongoe J (1996) Design guideline for continuous beams supporting steel joist roof structures. NASCC Proc
12. Slein R, Buth JS, Latif W, Kamath AM, Alshannaq AA, Sherman RJ, Scott DW, White DW (2020) Large-scale experimental lateral-torsional buckling tests of welded I-section members. In: Annual stability conference. Atlanta, GA, 1–20
13. Smith MD, Turner AK, Uang CM (2013) Experimental study of cyclic lateral–torsional buckling of web tapered I-beams. Department of Structural Engineering, University of California, San Diego, CA
14. Yarimci E, Yura JA, Lu LW (1967) Techniques for testing structures permitted to sway. Fritz laboratory reports (paper 112), Bethlehem, PA
15. Ziemian RD (2010) Guide to stability design criteria for metal structures. Structural Stability Research Council (SSRC), Wiley, Hoboken, NJ